

Leopard: Scaling BFT without Sacrificing Efficiency

*Kexin Hu, †Kaiwen Guo, ‡Qiang Tang, *Zhenfeng Zhang, †Hao Cheng, †Zhiyang Zhao

*Institute of Software, Chinese Academy of Sciences

†University of Chinese Academy of Sciences

‡The University of Sydney

{hukexin, kaiwen2016, zhenfeng, chenghao2020, zhiyang2018}@iscas.ac.cn

qiang.tang@sydney.edu.au

Abstract—With the emergence of large-scale decentralized applications, a scalable and efficient Byzantine Fault Tolerant (BFT) protocol of hundreds of replicas is desirable. Although the throughput of existing leader-based BFT protocols has reached a high level of 10^5 requests per second for a small scale of replicas, it drops significantly when the number of replicas increases, which leads to a lack of practicality. This paper focuses on the scalability of BFT protocols and identifies a major bottleneck to leader-based BFT protocols due to the excessive workload of the leader at large scales. A new metric of *scaling factor* is defined to capture whether a BFT protocol will get stuck when it scales out, which can be used to measure the performance of efficiency and scalability of BFT protocols. We propose “Leopard”, the first leader-based BFT protocol that scales to multiple hundreds of replicas, and more importantly, preserves a high efficiency. We remove the bottleneck by introducing a technique of achieving *constant* scaling factor, which takes full advantage of the idle resource and adaptively balances the workload of the leader among all replicas. We implement Leopard and evaluate its performance compared to HotStuff, the state-of-the-art BFT protocol. We run extensive experiments on the two systems with up to 600 replicas. The results show that Leopard achieves significant performance improvements both on throughput and scalability. In particular, the throughput of Leopard remains at a high level of 10^5 when the system scales out to 600 replicas. It achieves a $5\times$ throughput over HotStuff when the scale is 300 (which is already the largest scale we can see the progress of the latter in our experiments), and the gap becomes wider as the number of replicas further increases.

I. INTRODUCTION

Byzantine fault tolerance (BFT) protocols aim to enable a set of replicas to reach consensus, and endure arbitrary failures (a.k.a. *Byzantine faults*) from a subset of these replicas. As a fundamental primitive in distributed computing, it has been studied for decades in many classical works, e.g., [41], [51], [50], [15]. In general, BFT protocols reach consensus through several rounds of voting among all replicas. Two basic security properties are *safety* that honest replicas’ outputs are consistent, and *liveness* that honest inputs will be output by every honest replica.

BFT protocols have received a lot attentions showing substantial progress in both security [24], [27], [35] and efficiency [15], [11], [46], [31]. In particular, the optimal

resilience bound (1/3) of Byzantine fault while ensuring safety and liveness can be achieved simultaneously in the partially synchronous network model where a known bound of message transmission holds after some unknown global stabilization time (GST) [24]. Traditional BFT solutions that guarantee the two security properties while achieving the optimal resilience bound normally support for a small scale of replicas (e.g., a dozen replicas) with a moderate throughput (e.g., a few thousand operations per second) [15], [30], [2]. This is mostly due to the heavy communication cost in every voting round.

Since the emergence of decentralized applications on the Internet started from Bitcoin [47], even consortium blockchain may have a large number of peers (e.g., in a global supply-chain); moreover, BFT protocols are often adopted as an important component for the permissionless consensus (e.g., [25], [44], [37]) and proof-of-stake protocols (e.g., Algorand [28]), in which a large number of committee members (thousands) are chosen to run a BFT protocol. It follows that BFT protocols that can support a large number of replicas have become highly demanded. A practical BFT protocol should thus perform well on efficiency and scalability simultaneously, i.e., preserving a high throughput when the number of replicas increases¹.

Great efforts have been made to reduce the communication cost for improving scalability and efficiency. Current progress adopts the ideas such as cutting down the number of voting rounds [45], [39], lowering the number of required votes for each confirmation [1], [52], et al. While some of them achieving a better efficiency at the cost of weakening the ability to resist Byzantine faults [45], [1], [52], [39], there are major improvements recently that combine several optimization techniques both in protocol’s design and implementation, have realized a *linear* communication complexity without sacrificing the resilience ability [29], [58]. Evaluations show that they achieve a high throughput of confirming 10^5 requests per second [59].

Unfortunately, the latest evaluation results (Fig.1) of the state-of-the-art BFT proposals, HotStuff [58] and BFT-SMaRt [8], with at most 128 replicas show that the high throughput is only achieved on a small scale of replicas; when the number of replicas increases, the throughput drops sharply! It follows that those BFT protocols still face a scalability-efficiency dilemma.

BFT protocols are protocols that run on a distributed set of nodes. An intuitive idea to conquer the dilemma is to use

¹Algorand [28] provides a “scalable” BFT solution that supports thousands of nodes. However, the throughput is only about 1000, while we would like to have both scalability and high efficiency.

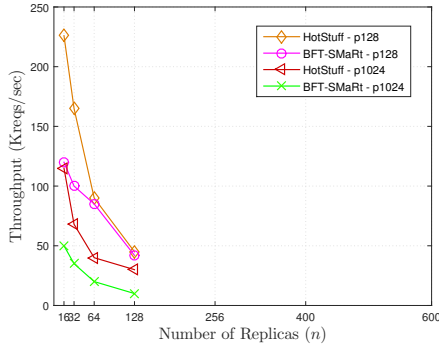


Fig. 1. Evaluation result [59] on the measure of throughput with different numbers of replicas in HotStuff [58] and BFT-SMaRt [8], under 128-byte and 1024-byte payload sizes.

two common methods in distributed systems for improving scalability and efficiency, namely *scaling out* (or horizontal scaling) and *scaling up* (or vertical scaling). One popular approach to design a “scale-out” system is by sharding [44], [37], [61]. By partitioning the replicas into multiple subsets (or shards) that each processes a disjoint set of pending requests in parallel, the processing capacity scales horizontally with the number of replicas. To endure Byzantine faults, replicas in each shard run a BFT protocol to confirm pending requests. However, to guarantee a secure confirmation in each shard, it is necessary for the BFT protocol to support a large scale (thousands) of replicas [23]. Therefore, a BFT protocol supporting large-scale replicas, while preserving high efficiency is still out of reach. Scaling up is to improve the efficiency of the protocol by adding more resources to each replica. Since resources are usually costly [5], [4], using scaling up to improve the protocol makes sense only if the efficiency’s improvement is significant. However, we find out (shown in §V) that the increased throughput in the state-of-the-art BFT protocols approaches 0 when the protocol’s scale is large.

These observations motivate us to consider the following main question of the paper:

Can we design a BFT protocol that is scalable (to at least several hundreds or more) and realizes a linear communication cost for most of the time, more importantly, preserves high efficiency and enables an effective scaling up?

A. Our Contributions

Most of the efficient BFT protocols (such as HotStuff) are leader-based constructions where a leader replica generates and disseminates consensus proposals (e.g., new blocks) each containing a bunch of requests to initiate the agreement. In this paper, we focus on scalable and efficient leader-based (partially synchronous) BFT protocols. Our contributions are three-fold:

Identifying the major bottleneck. The state-of-the-art BFT solutions have significantly reduced the communication cost of the protocol. They use techniques including vote aggregation (reduces the quadratic communication complexity caused by the all-to-all voting pattern to linear [58], [29]), a chained consensus ledger (simplifies the complicated Byzantine leader recovery mechanism [53], [16], [58]), the pipelined paradigm (reduces the average number of voting rounds to one for each confirmation [13]).

While those protocols mainly focus on reducing the cost of the protocol overall, one crucial but often neglected aspect in a leader-based BFT protocol is that the *leader* might be overloaded. To validate this in practice, we conducted an experimental evaluation of the leader’s workload² with an increasing number of replicas. The result in Fig. 2 shows that the leader’s workload increases dramatically as the protocol’s scale getting larger.

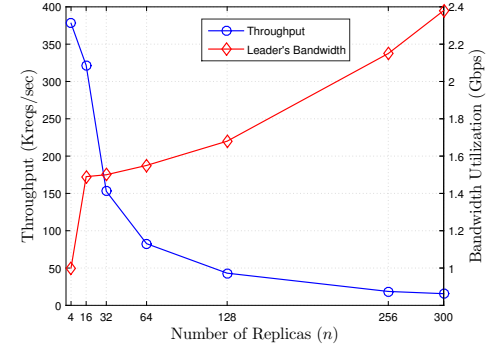


Fig. 2. Throughput and leader’s bandwidth usage of HotStuff [58] under 128-byte payload size.

Recall that the leader serves as disseminating every pending request in consensus proposals to all the other $n - 1$ replicas, and each non-leader replica only needs to process the requests received from the leader. Let Λ be the throughput (the number of requests confirmed per second) that we want to achieve, and *payload* denote the number of bits per request. As such, the workload of the leader during the dissemination for confirming Λ requests can be estimated by $\Lambda \times \text{payload} \times (n - 1)$, whereas a non-leader replica’s workload is $\Lambda \times \text{payload}$. Let C be the processing capacity, i.e. the number of bits that can be processed per second at each replica, and we have

$$\Lambda \times \text{payload} \times (n - 1) \leq C \quad (1)$$

holds for the leader³. Since a replica’s processing capacity is bounded by C , it comes that the achievable throughput will drop when n gets larger.

Therefore, to preserve the efficiency when the protocol’s scale increases, any replica’s workload should not become a bottleneck. To capture this, we define a performance metric called *scaling factor* to be the heaviest workload for confirming a bit of request among all honest replicas, i.e.

$$SF = \max_{1 \leq i \leq n} \{W_i\}.$$

where W_i denotes the workload of replica i .

Let’s take HotStuff as an example to evaluate the scaling factor (SF) of previous BFT solutions. Let W_{leader} (resp.

²We use the leader’s bandwidth utilization to indicate its workload since it can be easily measured. We chose HotStuff [58] as a typical example of the state-of-the-art leader-based BFT protocol to do the evaluation.

³A conventional optimization with engineering was running the consensus on the digest of requests to reduce the workload. However, this equals confirming requests with a lower payload size. The increase of leader’s workload with an increasing n still remains, and it cannot help to achieve a constant scaling factor (defined later).

$W_{\text{non-leader}}$) denotes the workload for confirming a bit of request at the leader (resp. a non-leader replica), and we have that

$$\begin{aligned} SF^{\text{pre}} &= \max\{W_{\text{leader}}^{\text{pre}}, W_{\text{non-leader}}^{\text{pre}}\} \\ &= \max\left\{\frac{\Lambda \times \text{payload} \times (n-1)}{\Lambda \times \text{payload}}, \frac{\Lambda \times \text{payload}}{\Lambda \times \text{payload}}\right\} \\ &= (n-1), \end{aligned}$$

which grows linearly with respect to the number of replicas n .

Usually, SF is a non-increasing function of n . Assume a replica's processing capacity is bounded by C , then the protocol's expected throughput is limited by C/SF , which will not increase with the growth of n . To preserve the throughput when the protocol's scale increases, it would be desirable to design a protocol that has a scaling factor that decreases slower, and in the ideal case, just a constant, and irrelevant to n !

In addition, scaling up the protocol by adding more resources to each replica is a common way to make a system perform better. Since C is the processing capacity per replica, the actual number of bits that can be confirmed per second is bounded by C , and we assume it equals to γC where the exact value of γ depends on the concrete protocol design but $\gamma \leq 1$ always holds. When scaling up the protocol, the processing capacity C will grow. However, to make the best use of the added resources when scaling up, γ should be a large value, and in the ideal case, approaching 1 (since $\gamma \leq 1$) and also irrelevant to n . From Eq.(1) we obtain that γ_{leader} in previous BFT solutions is bounded by $\frac{1}{n-1}$, which approaches 0 when n becomes larger. This leaves considerable room for improvement.

A scalable and efficient BFT. We present “Leopard”, a scalable and efficient BFT protocol in the partially synchronous network model. Leopard addresses the main question of the paper while ensuring safety and liveness without relaxing the optimal resilience bound: It preserves the efficiency when the protocol's scale increases, and it achieves the desirable scaling factor that is irrelevant to the scale of the protocol. Meanwhile, Leopard enables an effective scaling up with a constant $\frac{1}{2}$ improvement of throughput by doubling the configured resources. In addition, the communication complexity of Leopard is linear when the leader is honest, and the protocol features the hallmark of *optimistic responsiveness* [49]. The above characteristics make Leopard a desirable high-efficient leader-based BFT protocol. Let us briefly walk through the ideas.

Balancing the workload. The excessively unbalanced workload between the leader and each non-leader replica in most previous leader-based BFT protocols makes the leader be the “Achilles heel” of these protocols when the scale increases. In Leopard, it amortizes the leader's workload by taking full advantage of the idle resource of other replicas and balances the workload among all replicas.

To achieve this while preserving the leader-based BFT paradigm, we decouple a BFT consensus proposal into two planes: *Pending requests* and *indexes each to a package of pending requests*. Every non-leader replica packs the pending requests in its buffer and disseminates the package to all the others, whereby the leader only has to include an index to each outstanding package in consensus proposals.

By spreading the total $O(n)$ overhead during the request dissemination to $O(n)$ replicas, it enables that each replica's workload remains constant as the protocol's scale getting larger⁴. Every replica can receive all requests as before, which ensures that the subsequent confirmation on those requests will not be affected, and although it also introduces a vulnerability to Byzantine replicas, we discuss how to defend using the network-level technique from the existing literature [18]. Each index disseminated by an honest leader corresponds to a package of requests on which the leader has initiated an agreement among replicas. We instantiate the index by the use of the collision-resistant hash function to guarantee its uniqueness.

In this case, let α be the number of bits per package and β be the size of an index, and the scaling factor of Leopard is

$$\begin{aligned} SF^{\text{ours}} &= \max\{W_{\text{leader}}^{\text{ours}}, W_{\text{non-leader}}^{\text{ours}}\} \\ &= \max\{W_{\text{leader}}^{\text{ours-send}} + W_{\text{leader}}^{\text{ours-recv}}, W_{\text{non-leader}}^{\text{ours-send}} + W_{\text{non-leader}}^{\text{ours-recv}}\} \\ &\approx \max\{\beta \frac{\Lambda \times \text{payload}}{\alpha} \times (n-1) + \Lambda \times \text{payload}, \\ &\quad 2\Lambda \times \text{payload} + \Lambda \times \text{payload} \times \frac{\beta}{\alpha}\} / (\Lambda \times \text{payload}) \\ &= \max\{\frac{\beta(n-1)}{\alpha} + 1, 2 + \frac{\beta}{\alpha}\}. \end{aligned}$$

Note that, α is a parameter of the protocol satisfying $\alpha \geq 1$. When the scale of the protocol increases, we can adaptively adjust α with a larger value in order to counteract the effect by increasing n . Hence, the scaling factor of Leopard can remain constant as n increases, which achieves the ideal result of this metric.

Also, Leopard supports an effective scaling up with γ constant to $\frac{1}{2}$ for *all scales of the protocol*. It achieves a significant improvement that is substantially higher than the $\frac{1}{n-1}$ value of previous BFT solutions which approaches to 0 as n getting larger.

Further improvements of the protocol's design. Having the main advantage as stated above, we still need to make the remaining part of the protocol enable high efficiency and friendly to support a large scale of replicas.

In Leopard, an agreement is reached via two rounds of voting after it has been initiated by the leader. Each voting round collects sufficient $(\frac{2}{3}n+1)$ votes to avoid safety-violation by the potential 1/3 fraction of Byzantine faults. Agreements on different consensus proposals are executed in parallel to help to reduce the confirmation latency. Also, we leverage the known technique of threshold signature schemes [10], [54] to reduce the communication complexity during voting by one order of n . Each vote in Leopard is instantiated by a threshold signature share, while the proof for the completion of a voting round is an aggregated threshold signature that combines $\frac{2}{3}n+1$ threshold signature shares. When setting a collector to collect and distribute combined signatures, the communication complexity of the agreement step can drop to linear. Since there is no waiting for any extra delay for a normal agreement, it is optimistic responsiveness that in the optimistic

⁴Another common technique to balance the workload of a specific node on disseminating is reliable broadcast (RBC) with erasure codes. However, the quadratic communication complexity in existing schemes [14], [48], [22] is not friendly to support a large scale of replicas.

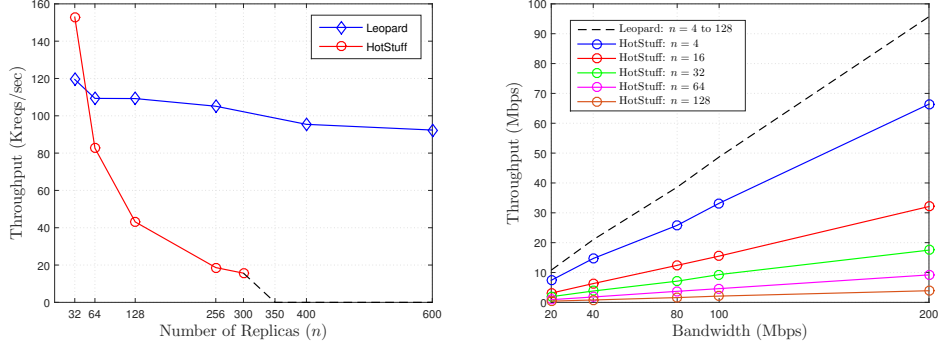


Fig. 3. Throughputs of Leopard and HotStuff when varying the number of replicas (left), or varying the configured bandwidth at each replica (right).

case of an honest leader, the protocol proceeds as fast as the messages can be delivered in the network.

For most of the time, the protocol processes and confirms requests under an honest leader, which is known as the normal-case mode. We still need a mechanism (a.k.a. the view-change) to replace the Byzantine leader and guarantee the liveness. By the use of threshold signature schemes, we can obtain a quadratic view-change solution instead of the cubic communication complexity in the traditional BFT protocols such as PBFT [15]. We emphasize the impact of the design choices in Leopard compared with the current BFT protocols with a linear view-change such as HotStuff [58]. HotStuff's agreement is limited in a sequential execution way via three voting rounds. Leopard allows a parallel-executed agreement with one less voting round, and hence it favors high efficiency in the normal-case mode, which mainly decides the efficiency of the protocol and happens most of the time.

Implementation and experimental evaluations. We design and implement a prototype BFT system based on Leopard. We evaluate its performance with up to 600 replicas. For a fair comparison, we deploy both Leopard and HotStuff back-to-back in the same environment of (c5.xlarge) Amazon EC2 instances. Since current HotStuff implementation by its authors [59] can hardly work when $n > 300$, we only compare the results of HotStuff with n up to 300.

Although the throughput of Leopard can be well preserved with an increasing package size α when n grows, the latency will decrease when α is getting larger. This is due to that more requests should be collected before a package is generated and a larger package can cost a longer time for delivery. Therefore, we balance the throughput and latency when choosing the package size⁵. Fig. 3 presents the main result of this paper. It shows that the throughput of Leopard remains almost flat and achieves around 10^5 for the replica number varies up to 600 (left in Fig. 3). Compared to HotStuff, Leopard achieves 5× throughput when n is 300, and the gap becomes wider with the growth of the scale. Meanwhile, we tested the effect of scaling up in both systems by adding the bandwidth from 20-200 Mbps at each replica, and the result (right in Fig. 3) shows that the throughputs of both systems grow proportionally. However, the growth rate of throughput in HotStuff approaches 0 as the scale getting larger, whereas Leopard remains at a high value

⁵In comparison, when using RBC with erasure codes like [14], the message size is bound by $\Omega(n \log n)$ due to the usage of erasure codes. This makes the tradeoff between throughput and latency impossible.

of about 1/2 with all tested scales. More details of the above two evaluations are shown in §V-B1 and §V-B3, respectively.

We further carry out a variety of experiments including the leader's bandwidth usage in both systems to compare their leaders' workloads (§V-B2), breakdowns about latency and network bandwidth (§V-B1 and §V-B2). In particular, to see the performance when the protocol suffers from a Byzantine leader, we evaluate the time and communication costs for a view-change with a varying n (§V-B4). The result shows that it costs less than 6 seconds for the completion of a view-change (measured from a view-change has been triggered to a new view has been started) when $n = 400$. This confirms that the complete protocol of Leopard will not get stuck like some other schemes (see Fig. 1) when the protocol's scale is large. It can work well when the scale of the system is at least hundreds.

B. Outline

We first present the preliminaries in §II. The protocol description is given in §III, followed by the analysis in §IV. §V gives the implementation and four types of experimental evaluations of Leopard. The further present a extensive comparison with some related work, which is shown in §VI. The paper is concluded in §VII.

II. PRELIMINARIES

A. Threat & Network Model

We consider a system consisting of a fixed set of $n = 3f + 1$ replicas, indexed by $i \in [n]$, where at most f replicas are Byzantine and others are honest. Each replica holds two signature key pairs (pk_i, sk_i) and (tpk_i, tsk_i) . The identities of replicas and their public keys are known to all. We will often refer to Byzantine replicas as being coordinated and fully controlled by an adversary. The adversary also knows the secret keys and internal states of all Byzantine replicas.

Partially synchronous network. Network communication among replicas is point-to-point, authenticated, and reliable. We adopt the partially synchronous network model of Dwork et al. [24], where a known bound Δ on message delivery holds after some unknown time point called the global stabilization time (GST). Time before GST is fully asynchronous with no bound on message delivery, i.e., the adversary can arbitrarily delay. Time after GST is synchronous. This model follows that of many BFT protocols, especially HotStuff [58] and PBFT [15].

B. Design goals.

We aim to design a leader-based BFT protocol that preserves high efficiency when the protocol's scale increases. It should satisfy the following efficiency and security goals under the above-defined threat and network model.

The efficiency goals. The efficiency goal of our protocol is measured by the following metrics⁶:

- *Constant scaling factor*: We require that the scaling factor of the protocol, i.e., the heaviest workload for confirming a bit of request among all replicas when they follow the protocol, is constant to n .
- *Optimistic responsiveness*: When the leader is honest and after GST, the confirmation latency of a request only depends on the actual network delay, rather than any known upper bound of the network delay.

The security goals. A secure BFT protocol satisfies the following two properties:

- *Safety*: The requests recorded in the same position of two output logs from honest replicas are identical.
- *Liveness*: A client request will eventually receive a response.

C. Cryptographic Notations.

We make standard cryptographic assumptions and we use the following cryptographic constructions. $H(m)$ is a collision-resistant cryptographic hash function, producing a hash value for the input message m . $\mathcal{S} = (\text{Sig}, \text{Vrf})$ is a regular signature scheme. $\text{Sig}(sk_i, m)$ is the signature algorithm on inputting secret key sk_i of replica i and message m , it outputs the corresponding signature σ_i . $\text{Vrf}(pk_i, \sigma_i, m)$ is the verification algorithm on inputting public key pk_i of replica i and signature-message pair (σ_i, m) , it outputs 1 if σ_i is a valid signature of m under sk_i ; otherwise, it outputs 0. $\mathcal{T}\mathcal{S} = (\text{TSig}, \text{TVrf}, \text{TSR})$ is a threshold signature scheme. $\text{TSig}(tsk_i, m)$ is the threshold signature algorithm on inputting secret key tsk_i of replica i and message m , it outputs the corresponding signature share $\hat{\sigma}_i$. $\text{TVrf}(tpk_i, \hat{\sigma}_i, m)$ is the verification algorithm on inputting public key tpk_i and signature-message pair $(\hat{\sigma}_i, m)$, it outputs 1 if $\hat{\sigma}_i$ is a valid threshold signature share of m under tsk_i ; otherwise, it outputs 0. $\text{TSR}(S)$ is the recovery algorithm on inputting a set S of $2f + 1$ valid signature shares of message m , it outputs a combined signature $\hat{\sigma}$. The combined signature $\hat{\sigma}$ can be verified by $\text{TVrf}(tpk, \hat{\sigma}, m)$ where tpk is the master public key of $\mathcal{T}\mathcal{S}$ which is known to all.

III. PROTOCOL OF LEOPARD

A. Overview

The protocol proceeds in successive views starting from 1. Each view consists of multiple agreement instances and a view-change. An agreement instance is for confirming a consensus

⁶In addition to constant scaling factor and optimistic responsiveness, we also want to have a protocol whose throughput's improvement is proportionally and significantly large to the added resources. Since it is hard to define a value to capture the effectiveness of scaling up, we omit its formal definition as an efficiency goal here. Nevertheless, an analysis of the effectiveness when scaling up the protocol is shown in §IV.

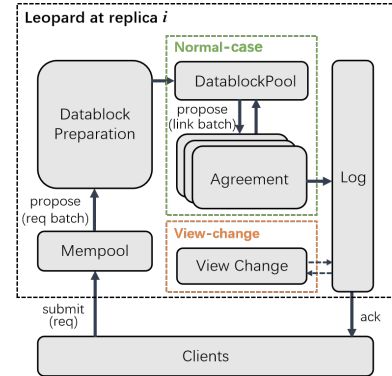


Fig. 4. The architecture of Leopard.

proposal proposed by the leader of the current view, and the view-change is for advancing to the next view. To preserve high efficiency when n increases, we decouple the heavy part of request dissemination from the agreement. Fig. 4 depicts the architecture of Leopard that features a memory pool (or *mempool*), a datablock preparation, a normal-case modular, a view-change modular, and a log. For most of the time, replicas execute the normal-case modular to confirm requests, a.k.a. the normal-case mode of the protocol. This happens as long as the current view leader is honest. Only if the leader is Byzantine, the view-change mode of the protocol is triggered and the view-change modular is executed by replicas to deal with the Byzantine leader.

The client submits pending requests to non-leader replicas and waits for $f + 1$ identical acknowledgments from replicas as a response. Since there are at most f replicas, a valid response must contain at least one acknowledgment from an honest replica which ensures the correctness of the response. The typical message flow (corresponds to the solid arrows in Fig. 4) is shown in Fig. 5.

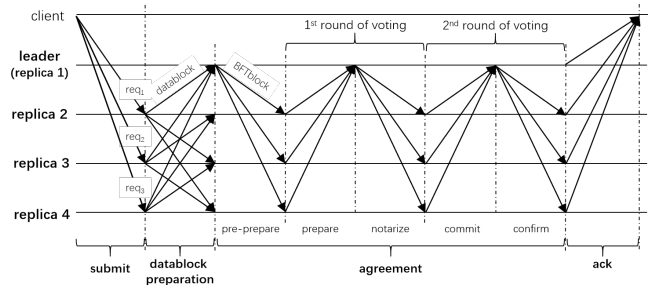


Fig. 5. The typical message flow of Leopard with $n = 4$.

Upon receiving requests from the client, each non-leader replica *continually* packs pending requests from its mempool to generate datablocks which are then sent to other replicas. As we try to balance the workload of replicas, we exclude the leader of the current view from generating datablocks but leave the work of initiating an agreement instance to the leader. The leader extracts datablocks that have passed a basic verification to generate a consensus proposal (or *BFTblock*), which is then sent to other replicas. Each agreement instance confirms a BFTblock by two rounds of voting among replicas. The decoupling of request dissemination from the agreement not only releases the tension of leader-based BFT protocols in the critical path (as stated in §I) but also benefits a parallel

execution of request's dissemination and confirmation which has not been reflected in Fig. 5.

To avoid the inconsistency of the output logs at different honest replicas which breaks safety, we assign each BFTblock a unique serial number and let replicas perform a uniqueness verification on each BFTblock before casting a vote. Since the network is partially synchronous, the order of messages received at a replica may not be consistent with the order they sent. To ensure high efficiency in spite of the disordered message delivery, a BFTblock in Leopard is allowed to be processed even if the former BFTblock has not started to process, and different BFTblocks can be processed in parallel to increase the processing rate. Notice that, every phase in an agreement instance is event-driven on the completion of its previous phase without waiting for any delay. This makes Leopard responsive during the normal-case mode.

As agreement instances are initiated by the leader, a Byzantine leader can obstruct the progress of the protocol by just being silent. Hence, we need a view-change mechanism to recover from this fault and reboot the normal-case mode at a new leader in the new view. This ensures the liveness of the protocol. As in [15], we let the client re-send the request that has not received a response for a long time after it has been submitted. This is to expose the potential Byzantine leader to every replica. A view-change is then triggered by a valid exposure of Byzantine behavior from the current leader.

B. Block Structure

Before presenting the detail of the protocol, we first define the newly introduced blocks: *datablock* and *BFTblock*.

(i) *Datablock*: A datablock is generated by a non-leader replica using requests from its mempool. The formation of a datablock is: $\langle \text{datablock}, \text{header}, \mathcal{R} \rangle$, where \mathcal{R} is a set of requests. Let $\text{header} := \langle i, (dgt, \text{counter}), \sigma_i \rangle$, where i denotes the identity of its generator, dgt is the digest of \mathcal{R} , counter shows the number of datablocks having been generated by i , and σ_i is a signature by i on the datablock.

(ii) *BFTblock*: The BFTblock is what replicas actually agree on. It is generated by the leader of the current view using received datablocks in its datablockPool. A BFTblock only contains the link (or hash) of the involved datablock. The formation of a BFTblock is: $\langle \text{BFTblock}, (v, sn), ct \rangle$, where v is the view number when creating the BFTblock, sn is the serial number assigned by the leader, and ct is the content of the BFTblock (i.e., links of datablocks). A BFTblock has two states: *notarized* and *confirmed*. A BFTblock is notarized if it has completed the 1st round of voting in an agreement instance, thus a corresponding *notarization proof* exists; a BFTblock is confirmed if it has completed the 2nd round of voting, thus a corresponding *confirmation proof* exists. Replicas change the state of BFTblocks on a valid proof's receival.

C. Protocol Description

Leopard is composed of a suite of tiered components to reach a consensus on pending requests. The output is a growing log of confirmed requests.

The protocol switches between two modes: the normal-case mode and the view-change mode. The normal-case mode is

designed to achieve agreements on requests lead by the current view leader. Each view has a unique leader known to all. The view-change mode is designed for replacing Byzantine leaders and advancing to the next view if a Byzantine leader appears.

We assume the current view number is v and denote the view leader as L_v . We now describe the protocol in a modular way that consists of datablock preparation, normal-case, and view-change.

■ **Datablock preparation.** Datablock preparation is to synchronize pending requests among replicas, completing the request dissemination with the help of every non-leader replica, thus balances the workload among replicas. Since the message delivery delay at different replicas may vary and in order to take full advantage of replicas, this process occurs on an ongoing basis and proceeds independently at each replica.

The algorithm for datablock's generation and verification is simple and shown in Algorithm 1. Every replica records a counter d initiated by 1. For each non-leader replica $i, i \in [n]$, it extracts requests from its mempool which stores pending requests collected from the client. i computes a hash value on the extracted set \mathcal{R} of requests as its digest dgt . A new datablock m is then generated with i 's signature on dgt and the current counter d . After m has been multicast, the counter increases by 1 indicating that a new datablock has been generated. On receiving a datablock m from replica i , the receiver puts m into its datablockPool if m contains a valid signature from i and no datablock with a repetitive counter has been received (line 18).

In a large-scale environment, geo-distributed replicas are likely to receive different requests from their neighbor clients, which makes the datablocks of a replica disjoint from others. However, a Byzantine replica may drop a received request to prevent it from being confirmed, i.e., censor the request. A client is thus allowed to send a request to s (at most $f + 1$) randomly chosen replicas. As about 1/3 fraction of replicas is Byzantine, a small $s = 9$ is sufficient to obtain an over 99.99% probability such that at least one replica is honest⁷. The honest replica will then guarantee the delivery of the request. To identify the responsible replicas for processing a given request req , each client can execute a deterministic function $\mu(req)$ which returns s identifiers of replicas. req is sent to those s replicas by the client, and every replica can also use $\mu(req)$ to evaluate whether to process req . A simple instantiation of $\mu(req)$ is by checking the equality of $H(req) \bmod q = H(i) \bmod q$, where $q = \frac{n-1}{s}$. In general, when setting $s = 1$, we can achieve the best possible performance since there is no repetition of requests among replicas. There is a tradeoff between higher efficiency and better fault resistance. A countermeasure to split the difference is to let the client send a request to s replicas only if no response has been received after it has been sent to a replica for a long period of time.

■ **Normal-case: agreeing on BFTblocks.** Requests are getting confirmed during the normal-case mode of the protocol. This is achieved by invoking agreement instances. An agreement instance consists of two-round voting by executing the normal-case protocol (see Algorithm 2), and multiple agreement instances each carrying a BFTblock can be conducted in

⁷The probability can be calculated by $Pr = 1 - (\frac{1}{3})^s$.

Algorithm 1 Datablock Generation & Verification

```

1: // Datablock generation
2: (for each non-leader replica  $i, i \in [n]$ )
3: Init:  $d \leftarrow 1$ 
4: while () do
5:   let  $\mathcal{R}$  be a set of requests extracted from its mempool
6:    $dgt \leftarrow H(\mathcal{R})$ 
7:    $\sigma_i \leftarrow \text{Sig}(sk_i, (dgt, d))$ 
8:   header  $\leftarrow \langle i, (dgt, d), \sigma_i \rangle$ 
9:    $m \leftarrow \langle \text{datablock}, \text{header}, \mathcal{R} \rangle$ 
10:  multicast  $m$  to all replicas
11:   $d \leftarrow d + 1$ 
12:  mempool  $\leftarrow \text{mempool} \setminus \mathcal{R}$        $\triangleright$  remove packed requests to
     avoid repetition
13: end while
14: // Datablock verification
15: (for all replicas)
16: upon receiving a datablock  $m$  from replica  $i$ 
17:    $dgt' \leftarrow H(m, \mathcal{R})$            $\triangleright$  check the integrity of content
18:   if  $\text{Vrf}(pk_i, m.\text{header}.\sigma_i, (dgt', m.\text{header}.d)) \rightarrow 0$  || (a valid
     datablock with the same  $d$  has been received from  $i$ ) then
19:     return reject
20:   else                                 $\triangleright$  the datablock is valid
21:     datablockPool  $\leftarrow \text{datablockPool} \cup \{m\}$ 
22:   return accept
  
```

parallel. This enables handling new requests without waiting for the completion of previous ones. We limit the number of parallel-executed BFTblocks to k , in case a Byzantine leader picks a number that is so high to exhaust the space of serial numbers. As in [15], we set a lower watermark lw and a higher watermark $lw+k$ to limit the region of a valid serial number of BFTblock. Since k can be large enough and the parameter lw will be advanced (due to the checkpoint mechanism introduced below), the process of agreeing will not stall waiting for the completion of previous BFTblocks, thus the parallel execution will be maintained.

In the protocol, BFTblocks are processed (lines 2-40) in parallel. Since a BFTblock contains links (or *hashes*) to datablocks and a datablock contains requests, the confirmation of a BFTblock is equivalent to the confirmation of all its linked requests. Once a BFTblock is confirmed at replica i , i will store the BFTblock in its local log following the order of m 's serial number. Hence the corresponding requests are also logically stored in the log, where requests linked by a BFTblock can be ordered in alphabetical order.

Instead of the all-to-all voting pattern as in [15] which brings a quadratic communication complexity, we adopt the threshold signature scheme \mathcal{TS} to reduce the communication complexity to linear. Letting each vote be a signature share generated by the TSig algorithm (lines 6, 18, and 29), a (notarization/confirmation) proof of a BFTblock can be generated by the TSR algorithm on inputting sufficient (i.e., $2f+1$) shares to obtain a combined signature (lines 23 and 35). Due to that the replica that combines votes is critical for the completion of the agreement, we let the leader do this job since a Byzantine leader will be replaced anyway (by the view-change protocol below).

Response to the client: As BFTblocks are processed in parallel agreement instances, the order of their confirmations may not follow the order of the serial numbers, and the confirmation

Algorithm 2 Agreeing on BFTblocks

```

1: Init:  $sn \leftarrow 1; lw \leftarrow 0$ 
2: // Pre-prepare stage
3: (for leader  $L_v$ )
4:   let  $ct$  be a set containing the hashes of outstanding datablocks
5:    $m \leftarrow \langle \text{BFTblock}, (v, sn), ct \rangle$        $\triangleright$  generate a BFTblock  $m$ 
6:    $\hat{\sigma}_{L_v}^1 \leftarrow \text{TSig}(tsk_{L_v}, H(m))$   $\triangleright$  sign the hash of  $m$  with  $tsk_{L_v}$ 
7:   multicast  $(m, \hat{\sigma}_{L_v}^1)$  to all replicas
8:    $sn \leftarrow sn + 1$ 
9: // Prepare stage
10: (for replica  $i, i \in [n]$ )
11: if the received  $(m, \hat{\sigma}_{L_v}^1)$  satisfies:  $\triangleright$  exclude invalid BFTblock
    -  $\text{TVrf}(tpk_{L_v}, \hat{\sigma}_{L_v}^1, H(m)) \rightarrow 1$ ;
    -  $v$  is the current view number;
    - no other BFTblock with the same  $sn$  has been voted in  $v$ ;
    -  $lw < sn \leq lw + k$        $\triangleright$  limit the outstanding BFTblock
      number to  $k$ 
12:   - each item in  $m.ct$  corresponds to a datablock in its datablock-
     Pool;       $\triangleright$  all linked datablocks have been received and are
     valid
13:   then
14:      $\hat{\sigma}_i^1 \leftarrow \text{TSig}(tsk_i, H(m))$        $\triangleright$  generate  $i$ 's signature share
15:     send  $(H(m), \hat{\sigma}_i^1)$  to  $L_v$            $\triangleright$  first-round vote
16: // Notarize stage
17: (for leader  $L_v$ )
18:   wait for  $2f+1$  valid signature shares for  $H(m)$ 
19:    $\hat{\sigma}^1 \leftarrow \text{TSR}(\{\hat{\sigma}_j^1\}_{j=1}^{2f+1})$        $\triangleright$  the notarization proof for  $m$ 
20:   multicast  $(H(m), \hat{\sigma}^1)$  to all replicas
21: // Commit stage
22: (for replica  $i, i \in [n]$ )
23: if  $\text{TVrf}(tpk, \hat{\sigma}^1, H(m)) \rightarrow 1$  then
24:   change the state of  $m$  to notarized
25:    $\hat{\sigma}_i^2 \leftarrow \text{TSig}(tsk_i, H(\hat{\sigma}^1))$ 
26:   send  $(H(\hat{\sigma}^1), \hat{\sigma}_i^2)$  to  $L_v$            $\triangleright$  second-round vote
27: end if
28: // Confirm stage
29: (for leader  $L_v$ )
30:   wait for  $2f+1$  valid signature shares for  $H(\hat{\sigma}^1)$ 
31:    $\hat{\sigma}^2 \leftarrow \text{TSR}(\{\hat{\sigma}_j^2\}_{j=1}^{2f+1})$        $\triangleright$  the confirmation proof for  $m$ 
32:   multicast  $(H(\hat{\sigma}^1), \hat{\sigma}^2)$  to all replicas
33: (for replica  $i, i \in [n]$ )
34: if  $\text{TVrf}(tpk, \hat{\sigma}^2, H(\hat{\sigma}^1)) \rightarrow 1$  then  $\triangleright$  complete the confirmation
35:   change the state of  $m$  to confirmed
36:   add  $m$  into  $i$ 's log following the order of  $m$ 's serial number
  
```

order at different replicas may also differ. This can happen even the current leader is honest since the network is partially synchronous. However, the execution of requests must follow a sequential order at each replica to obtain a consistent execution state. Therefore, we require that only the confirmed BFTblocks (i.e., the linked requests) with sequential serial numbers can be executed. In spite of this, to let the protocol well suited for different requirements in applications, there are two options of when to create an acknowledgment for the client: If the request needs a fast response as in some fast payment application, a replica can send the acknowledgment as long as the BFTblock has been confirmed, since a confirmed BFTblock will be executed anyway (show in the proof for safety); otherwise, if the client needs to know the final execution state, the acknowledgment can only be created until the BFTblock having been executed.

■ **Normal-case: making checkpoints.** To reduce the storage

overhead of replicas, a.k.a., the garbage collection, it would be better if we could remove all executed requests from the buffer. As in [15], [29], we periodically (every $k/2$) invoke a checkpoint protocol on the latest executed BFTblock, denoted as B . The generation of a valid checkpoint is a one-round voting process. In this way, the requests related to every BFTblock with the serial number lower than B 's can be removed from the buffer. Meanwhile, we advance the lower watermark lw in Algorithm 2 to the serial number of B . Due to the space limitation, we leave the detailed checkpoint protocol to appendix A.

■ View-change: replacing Byzantine leaders. The view-change aims to replace Byzantine leaders and reboot the normal-case mode at a new leader in the next view. The protocol contains three steps: view-change trigger, leader rotation, and state synchronization. View-change trigger decides when to invoke the view-change protocol. Leader rotation appoints the identity of the new leader. State synchronization synchronizes the state of the current view among replicas to avoid safety-violation in the new view.

We adopt a simple round-robin policy as in [17], [29], [36] for the leader election, where the $(v \bmod n)$ -th replica is the eligible leader of view v . The view-change trigger and state synchronization steps in Leopard are similar to PBFT [15]. A view-change is triggered by a time-out request. Once the client finds out a request that has not received a response for a long period of time after its submission, the client resends the request, with a special tag on it, to non-leader replicas which are then disseminated within datablocks as a normal request. However, a timer will be set at each replica on receiving a time-out request. And if the timer expires before the request being confirmed, the view-change progress is triggered. After that, each replica sends a new-view message, containing every notarized and confirmed BFTblock (together with its proof) whose serial number is larger than lw , to the next view leader L_{v+1} . Once $2f+1$ valid new-view messages have been received, L_{v+1} collects them and multicasts to other replicas. When replicas receive a valid response from L_{v+1} , they advance to view $v+1$ by first redoing the agreement for each BFTblock contained in the response. More details about the view-change protocol are deferred to appendix A.

Remarks: We discuss some potential malicious behaviors and the corresponding defenses with the help of common network-level techniques. For a Byzantine replica, it may try to deliver conflict datablocks with the same counter and cause an inconsistency among replicas, or refuse to send datablocks to some specific replicas. However, since Leopard is a leader-based BFT protocol, the content of each agreement instance is decided by the leader. As such, only the datablock received by the leader will be confirmed. Also, a missing datablock can be obtained via sending a request to ask the leader for the datablock. Since each datablock contains the identity of its generator, together with a counter, the malicious behavior of the Byzantine replica can be detected by others. Also, the counter in the datablock can be used to limit the number of datablocks received from a replica, which is a common balancer-aware strategy of throttling to prevent network-level attacks (e.g., DoS) [18], [42] or exhausting the space of numbers.

We note that this paper focuses on reaching consensus

among replicas like many other BFT protocols [15], [46], [58], it doesn't check the validity of the request. When the protocol is applied to some application scenarios, an application-specific verification function `verify()` should be invoked to verify client requests before casting the first round of voting. Since we require the receipt of linked datablocks before casting a vote (line 16 in Algorithm 2), the verification can be directly added in the protocol. Also, a similar technique as in [19] can be used to reconcile conflicted requests before the output.

In addition, the communication complexity of the view-change in current protocol is quadratic (see §IV), the same as PBFT and LibraBFT [7]. However, one can also use our technique of decoupling on top of the scheme like HotStuff to enjoy its linear view-change. We emphasize that this, however, will lose the parallel execution as in Leopard (see §VI).

IV. ANALYSIS

Efficiency analysis. In this part, we analyze the two main efficiency goals of our protocol, namely scaling factor and optimistic responsiveness. We also give an analysis of the effectiveness when scaling up the protocol.

Recall that, the optimistic responsiveness requires the confirmation latency of a request only depends on the actual network delay δ rather than any known upper bound of the message delay, if in the optimistic case that the leader is honest and after GST. The protocol is optimistic responsiveness because there is no waiting for any extra delay in the normal-case mode as depicted in Algorithm 2 and Fig. 5. In this optimistic case, it will cost 7δ before a request being confirmed after being submitted by the client, where δ is the network delay after GST.

Next, we analyze the scaling factor of our protocol. To simplify the analysis, we first focus on the heavy part related to request dissemination. Notice that when all replicas follow the protocol, the view-change protocol will not be triggered. In the best case that datablocks are disjoint, the workload of request dissemination will be amortized evenly by the $n-1$ non-leader replicas. Let Λ_r be the total number of pending requests, and payload denote the payload size per request. Hence, each non-leader replica will process $\frac{\Lambda_r \times \text{payload}}{n-1}$ bits of requests.

Let α be the number of bits per datablock and β be the size of a hash value. When processing Λ_r requests, it will generate $\frac{\Lambda_r \times \text{payload}}{\alpha}$ datablocks in total. Since a BFTblock only contains the hashes of datablocks, we have that the total bits of corresponding BFTblocks will be $\frac{\Lambda_r \times \text{payload}}{\alpha} \times \beta$.

According to the protocol, a leader receives datablocks from $n-1$ non-leader replicas, generates and sends BFTblocks to others. Hence, the leader's workload \bar{W}_L is estimated by,

$$\begin{aligned} \bar{W}_L &= \bar{W}_{\text{leader}}^{\text{recv}} + \bar{W}_{\text{leader}}^{\text{send}} \\ &= \frac{\Lambda_r \times \text{payload}}{n-1} \times (n-1) + \frac{\Lambda_r \times \text{payload}}{\alpha} \times \beta \times (n-1) \\ &= \left(\frac{\beta(n-1)}{\alpha} + 1 \right) \cdot (\Lambda_r \times \text{payload}). \end{aligned}$$

For each non-leader replica, it will first receive $\frac{\Lambda_r \times \text{payload}}{n-1}$ bits of requests from the client. It then sends the generated $\frac{\Lambda_r \times \text{payload}}{\alpha}$ datablocks to other $n-1$ replicas including the

leader, and receives datablocks from other $n - 2$ non-leader replica. The replica also receives BFTblocks send from the leader. Hence, a non-leader replica's workload \bar{W}_R is estimated by

$$\begin{aligned}\bar{W}_R &= \bar{W}_{\text{non-leader}}^{\text{recv}} + \bar{W}_{\text{non-leader}}^{\text{send}} \\ &= \frac{\Lambda_r \times \text{payload}}{n-1} + \frac{\Lambda_r \times \text{payload}}{n-1} \times (n-1) \\ &\quad + \frac{\Lambda_r \times \text{payload}}{\alpha} \times \beta + \frac{\Lambda_r \times \text{payload}}{n-1} \times (n-2) \\ &= (2 + \frac{\beta}{\alpha}) \cdot (\Lambda_r \times \text{payload}).\end{aligned}$$

From the above, we have that the scaling factor, i.e., the heaviest workload for confirming a bit of request among all replicas when following the protocol, can be estimated by

$$\begin{aligned}SF &= \max\{\bar{W}_L, \bar{W}_R\}/\text{payload} \\ &= \max\{\frac{\beta(n-1)}{\alpha} + 1, 2 + \frac{\beta}{\alpha}\}.\end{aligned}$$

Notice that, α is a system parameter denoting the datablock size. When we let $\alpha = \lambda(n-1)$ where λ is a constant positive number, then we can have a constant SF with respect to n . While if in the case that the client sends a request to s replicas to avoid Byzantine replica's censorship, the request will be repetitively disseminated at most s times. This makes each replica's workload increase by a factor of s . As long as s is constant (which has been discussed in §III), the increase of the workload will not impede the protocol to achieve a constant scaling factor.

We then evaluate the workload after the agreement has been initiated. Since the workload is mainly for the two-round voting for each BFTblock and each BFTblock links to at least one datablock, we have that the workload for the leader is no more than $\frac{\Lambda_r \times \text{payload}}{\alpha} \times 4\theta \times (n-1)$ on both receiving and sending votes. Since each non-leader replica's only has to send votes to the leader, its workload can be estimated by $\frac{\Lambda_r \times \text{payload}}{\alpha} \times 4\theta$. When the size of a datablock $\alpha = \lambda(n-1)$, we have that the heaviest workload among replicas remains constant to n .

Now we give an analysis of the effectiveness when scaling up the protocol. When adding more resources to each replica, the processing capacity is increased. Let Λ_b^Δ denote the increased bits of requests that can be processed by the protocol, and W^Δ denote the increased workload on dealing with Λ_b^Δ bits. If $\beta < \lambda$ is satisfied, we have that $\frac{\beta(n-1)}{\alpha} = \frac{\beta(n-1)}{\lambda(n-1)} < 1$. Usually, β is in dozens of bytes and a request is in hundreds of bytes. When the protocol scales to a large number like several thousand, we have that each datablock should contain several hundreds of requests in order to satisfy the condition $\beta < \lambda$. We emphasize that the block in many existing consensus protocols already contains hundreds of requests [32], which means $\beta < \lambda$ can be well satisfied. Hence, $\beta \ll \alpha$ is also holds with a large n since $\alpha = \lambda(n-1)$. From the above, we

deduce that

$$\begin{aligned}\frac{\Lambda_b^\Delta}{W^\Delta} &= \frac{\Lambda_b^\Delta}{\Lambda_b^\Delta \times \max\{W_L, W_R\}} \\ &= \frac{1}{\max\{\frac{\beta(n-1)}{\alpha} + 1, 2 + \frac{\beta}{\alpha}\}} \\ &= \frac{1}{2 + \frac{\beta}{\alpha}}\end{aligned}$$

which is about 1/2. Therefore, Leopard enables scaling up with 1/2 improvement of throughput by doubling the configured resources.

Remark: We didn't consider some excessive malicious conditions here as discussed in §III-C since this paper mostly focuses on the efficiency of the protocol in the normal-case. We note that the considered malicious conditions can be resolved by common network-level solutions.

Communication complexity analysis. According to the above analysis, the communication cost of the leader is $(\frac{\beta(n-1)}{\alpha} + 1 + \frac{4\theta(n-1)}{\alpha}) \cdot (\Lambda_r \times \text{payload})$ during the normal-case mode. For the case $\alpha = O(n)$, we obtain that the communication complexity of the leader is $O(1)$. The communication cost of each non-leader replica is $(2 + \frac{\beta}{\alpha} + \frac{4\theta}{\alpha}) \cdot (\Lambda_r \times \text{payload})$, thus its communication complexity is $O(1)$. Since there are $O(n)$ non-leader replicas in total, the communication complexity of the protocol in the normal-case mode is $O(n)$.

In the view-change mode, the new view leader should collect $(\frac{2}{3}n + 1)$ new-view messages, each contains at most k BFTblocks where k is constant. These messages will then send to n replicas, which makes the communication complexity of the protocol in the view-change mode be $O(n^2)$.

Security analysis. Leopard satisfies safety, captured in Theorem 1, and liveness, captured in Theorem 2. Since the proofs of safety and liveness are similar to that of PBFT [15], we defer the proofs for the following theorems to appendix B.

Theorem 1 (Safety). *If two distinct requests exist on the same position of two output logs, then the two logs cannot be both from honest replicas.*

Theorem 2 (Liveness). *After GST, the confirmation for a client request must be completed.*

V. IMPLEMENTATION & EVALUATION

A. Implementation

We have implemented a prototype of Leopard in Golang within roughly 5,600 lines of code. The system architecture is illustrated in Fig. 6. We encapsulate the mechanism for ensuring safety and liveness in a modular approach.

The system can be divided into seven modules: *Execution engine* is to pass a newly received message to the following modules for verification and it casts votes on valid messages. *Block manager* is mainly to verify the validity of blocks with the help of cryptographic algorithms provided by *crypto toolkit*. *Block pool* is to store outstanding blocks. *Log manager* is to record notarized of confirmed BFTblocks. *View transfer* is to do the view-change. *Reliable and authenticated channel* is for transmitting messages to/from others.

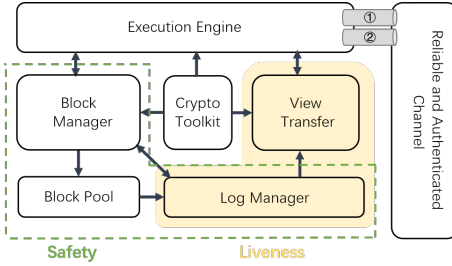


Fig. 6. Architecture of Leopard implementation.

Since a high throughput and a large scale of replicas are expected, there will be a large number of message exchanges. To avoid a frequent handshake between replicas which may affect the performance, we realize the communication channel by a point-to-point HTTP persistent connection based on TCP [57]. Notice that the heaviest part of the communication is from the datablock dissemination, but the one that decides an agreement is for the BFTblock (and its votes). We use two channels in Golang to process BFTblocks (channel ①) and datablocks (channel ②), respectively. To avoid congestion from datablocks, we set messages via channel ① a higher priority when processing. It ensures the progress of the agreement.

B. Experimental Evaluation

In the below, we show that our implementation of Leopard preserves a high throughput of 10^5 when it scales to 600 replicas. We compare the performance of Leopard to HotStuff, its closest competitor, using the implementation by its authors [60]. Since we mainly focus on the consensus, we only evaluated the performances of both systems without any application-specific verification of requests. We emphasize that there are several other systems like BFT-SMaRt [8], Tendermint [11] and SBFT [29]. However, to save the cost for large-scale experiments, we only compare with the state-of-the-art solution, HotStuff.

We ran four types of experiments, all with the number of Byzantine replicas to the largest possible one (i.e., touching the $1/3$ optimal resilience bound). This is for testing the performance with the highest achievable fault tolerance: (i) we varied the number of replicas up to 600 to evaluate the scalability (§V-B1); (ii) we evaluated the bandwidth usages on a varying n (§V-B2); (iii) we varied the configured bandwidth on each replica to evaluate the effectiveness of scaling up (§V-B3); (iv) we further evaluated the time and communication costs on the view-change of Leopard (§V-B4).

The experiments were conducted on Amazon EC2 virtual machine (c5.xlarge) instances, each has 4 vCPUs and less than 9.8 Gbps TCP bandwidth measured by *iperf* among several randomly selected instances. We ran each replica on a single EC2 instance. All the EC2 instances are connected via a point-to-point network. Every experimental result is averaged over 3 runs, each lasting until the measurement is stabilized.

1) *Scalability*: To compare the scalability of the two systems, we examined the throughput and latency with a fixed 128-byte payload size and an increasing number of replicas. This shows how fast they could go. We measured the latency as the time elapsed from the client submitting the request to having received $f + 1$ valid acknowledgments. This captures the time

used for a request from its generation to its finalization and no other measurement leads to a longer result. The throughput is measured from the leader's side. Since the leader in both systems generates the confirmation proof and sends it to other replicas, the leader will output ahead of others. This seems that the throughput measured from the leader may be higher than measured from other replicas. However, our evaluation result is an average of several runs each was collected when the system had been stabilized. We observed that the two measurement results are almost the same.

Intuitively, increasing the block batch size can better amortize the cost and leads to a higher throughput. However, a larger batch size will result in an increase of the latency since it should wait for more requests and a longer time will be spent to deliver a large block. Therefore, we first measured the throughput and latency on varying the batch sizes with 32-600 replicas. Results show that throughput goes up as we increase the batch size, but it almost stops growing after a certain batch size value. This confirms that the throughput cannot be improved just by setting a larger batch size, the same as in other works [19], [59], [11]. The latency keeps increasing when the batch size gets larger. Hence, we chose the batch sizes after balancing the throughput and latency. The detailed result is shown in appendix C and Table I presents the batch sizes we used in all the following experiments.

TABLE I. IMPLEMENTATION PARAMETERS.

n	Batch sizes in Leopard		Batch size in HotStuff
	datablock size	BFTsize*	
32	2000	100	800
64	2000	100	800
128	3000	300	800
256	4000	300	800
300	—	—	800
400	4000	400	—
600	4000	400	—

* BFTsize denotes the batch size of a BFTblock.

Fig. 7 depicts throughput (left figure) and latency (right figure) of Leopard and HotStuff. Since the current HotStuff implementation can hardly work when $n > 300$, Fig. 7 only shows the result with n up to 300. It shows that the throughput of Leopard drops only slightly and remains almost flat when n varies up to 600. Leopard achieves a $5\times$ throughput when $n = 300$ compared to HotStuff, and the gap gets wider when n increases. The latencies of both systems share the same tendency as n increases. However, the latency of Leopard is higher than HotStuff for all tested n . This is because when using batch sizes in Table I, the number of requests processed by a BFTblock (i.e., datablock size \times BFTsize) in Leopard is larger than the number in a HotStuff block. Hence, Leopard spends a longer time collecting enough requests. However, HotStuff suffers from a significant drop in throughput when its scale increases. Despite that, the latency of Leopard is good with a small scale (e.g., less than 1.5 seconds with $n \leq 32$).

To further evaluate the latency, we broke the latency down and measured the usage of time on different steps during an agreement in Leopard's implementation. The result in Table II shows that, Leopard's implementation costs over 60% on the datablock preparation. In particular, over 50% is spent on the dissemination of datablocks. This means that dissemination

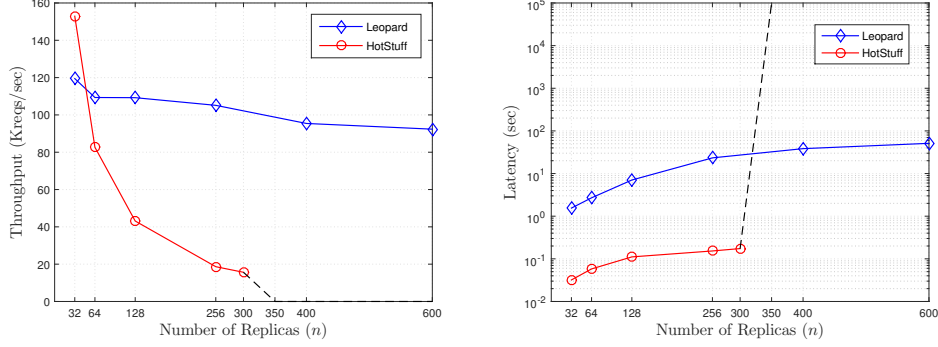


Fig. 7. Scalability of Leopard and HotStuff.

dominates the latency. It indicates the correctness of our design concept, i.e., to allow replicas disseminating datablocks on an ongoing basis without being impeded by each other which makes full use of the resource. We note that various engineering optimizations like parallel TCP connections, more aggressive TCP congestion control strategies and parallelization for validating burst incoming data can further optimize the current implementation. We leave it as our future work.

TABLE II. LATENCY BREAKDOWN OF LEOPARD WITH $n = 32$.

Usage		%Latency
Datablock Preparation	Datablock Generation	12.98%
	Datablock Dissemination	50.30%
	SUM	63.28%
	Agreement	35.97%
Response to the Client		0.75%

2) *Bandwidth usage*: Since the leader's overhead is the major bottleneck in existing leader-based BFT protocols, we evaluate the leader's bandwidth usage for both systems, and the result is depicted in Fig. 8. It shows that the leader's bandwidth usage in Leopard has been greatly reduced to lower than 0.5 Gbps for all tested scales, where the bandwidth usage of HotStuff rises rapidly when n increases.

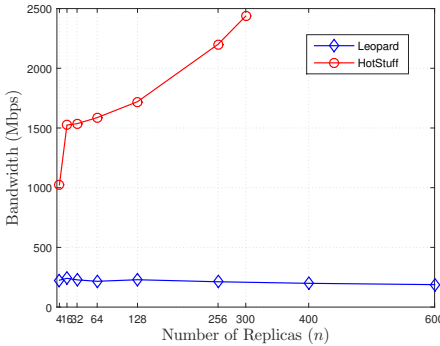


Fig. 8. Bandwidth usage of the leader in Leopard and HotStuff.

We further evaluate the bandwidth usage breakdown at the leader and the non-leader replica in Leopard. Table III presents the result with $n = 32$. Most of the bandwidth at the leader (over 96%) is used on receiving datablocks, whereas the cost on sending BFTblocks is only 3.17%. For each non-leader replica, most of the bandwidth is used on sending/receiving datablocks and the cost of sending messages is a little higher than receiving. This is due to that it sends a datablock to $n - 1$

other replicas but only receives $n - 2$ replicas' datablocks (since the leader is excluded from generating the datablock). Notice that the bandwidth used on receiving requests (both from other replicas and the client) takes up about 50% bandwidth usage at a non-leader replica. Since the throughput is limited by the number of requests received per second, this indicates that the effective network bandwidth usage ratio is 1/2 in Leopard. Moreover, just a small percentage (less than 1%) of bandwidth is spent on dealing with votes. This confirms that using vote-complexity to measure the efficiency of a leader-based BFT protocol as in previous works is defective.

TABLE III. BANDWIDTH USAGE BREAKDOWN OF LEOPARD.

Role	usage	%Bandwidth	
Leader	Sent	Consensus Proposal	3.17%
		Vote Result/Proof	0.24%
		Miscellaneous	0.15%
	SUM	3.56%	
	Received	Datablock	96.17%
		Vote	0.16%
		Miscellaneous	0.10%
	SUM	96.44%	
Non-leader Replica	Sent	Datablock	49.93%
		Vote	0.01%
		Miscellaneous	0.05%
		SUM	49.99%
	Received	Consensus Proposal	0.05%
		Datablock	48.34%
		Vote Result/Proof	0.01%
		Reqs. from Clients	1.61%
	SUM	50.01%	

3) *Effectiveness of Scaling Up*: A common way in practice to make a system perform better is to configure with more physical resources, a.k.a, scaling up the system. A natural question is: whether the throughput's drop can be mitigated or even conquered by configuring with more resources. We evaluate how Leopard and HotStuff perform with an increasing available bandwidth at each replica to verify this conjecture.

We throttled the available bandwidth at each replica from 20 to 200 Mbps using NetEm [43]. Fig. 9 depicts the throughput under different available bandwidths for both Leopard and HotStuff with a varying n . For all tested scales, the throughput grows proportionally with the available bandwidth. Therefore, the throughput of both Leopard and HotStuff can be improved by configuring with more bandwidth resources. However, when n becomes larger, the ratio of increased throughput over the

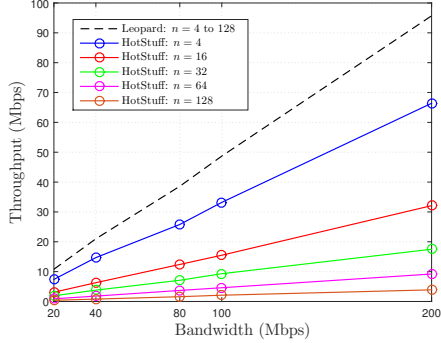


Fig. 9. Throughput with different available bandwidths at each replica in Leopard and HotStuff.

increased bandwidth approaches 0 in HotStuff. This means that the throughput of HotStuff cannot be improved effectively under a large n , which indicates the above conjecture is wrong. As a comparison, the effective network bandwidth usage ratio of Leopard remains at about 1/2. This is consistent with the result in §V-B2. Because of the significant difference for all tested scales, we conclude that the effectiveness when scaling up Leopard is significantly superior to HotStuff.

4) *View Change*: It is generally conjectured that the heavy view-change may hinder the support for large-scale replicas. Meanwhile, a Byzantine leader can obstruct the confirmation of request and decreases the efficiency of the system by letting the protocol switch to the view-change mode. In this part, we measure the performance of the view-change in Leopard with up to 400 replicas to evaluate its time and communication costs. The result is measured after a view-change has been triggered since the expired time for triggering a view-change may vary in different applications. In our evaluation, we randomly stop the leader to trigger a view-change.

Fig. 10 depicts the results. It shows that when the protocol's scale increases, both the time and total communication cost increase. However, when the protocol scale goes up to hundreds (400), the time cost of a view-change state synchronization period can be still in seconds (less than 6s). The total communication cost when $n = 400$ is less than 100MB, and most of the communication cost is produced by the leader (for sending a new-view message that contains $2f + 1$ view-change messages to all n replicas). In addition, since the view-change is triggered randomly in this experiment, the number of pending BFTblocks varies and this leads to a varied evaluation result in different runs.

We note that the cost on a view-change is mainly for processing BFTblocks that are not included in the latest checkpoint. Although the view-change protocol of Leopard is mostly based on PBFT, the number of pending BFTblocks could be small since the number of requests linked by a BFTblock in Leopard is large. This helps to reduce the cost of a view-change. Also, since the view-change only happens occasionally, the above evaluation result indicates that Leopard can work well when the scale of the system is in hundreds.

VI. RELATED WORK

Reaching consensus in the face of Byzantine failures was first introduced by Lamport et al. in the 1980s [50], [41].

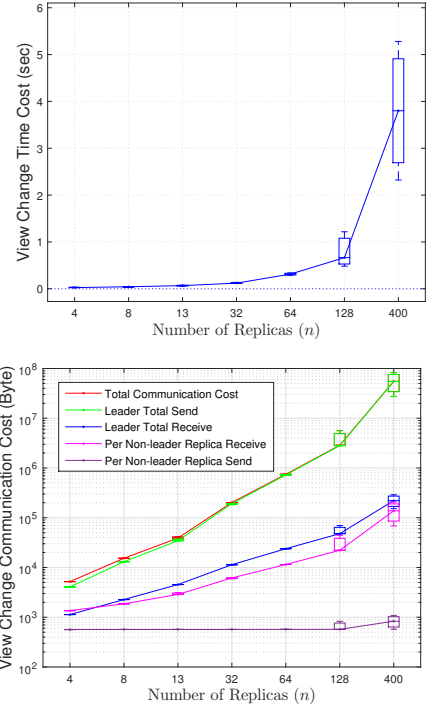


Fig. 10. View-change time and communication costs of Leopard's implementation.

Early BFT protocol that preserves safety and liveness in the partially synchronous network model is present by Dwork et al. [24] with a $O(n^4)$ communication complexity. The first practical BFT protocol in history is the seminal work of PBFT [15]. Its pioneering idea of three-phase and two-round voting initiated by a leader inspires many other works along this line of research. However, it suffers from the well-known communication drawback during the agreement: the $O(n^2)$ communication complexity mostly due to its all-to-all communication pattern.

While great efforts have been made on the way to reduce the quadratic communication complexity, SBFT [29] and HotStuff [58] use cryptography, especially the threshold signature scheme [54], [20], [10], [9], to allow a single message acknowledgment rather than $O(n)$ messages for each decision. This effectively reduces the communication complexity by one order of n , which achieves a linear communication complexity when the leader is honest. Experimental evaluations [59] also shown that the scalability and efficiency have been improved significantly, from supporting only tens of replicas as in PBFT to over one hundred, and it can achieve a peak throughput over 10^5 . Our protocol leverages this idea to obtain a linear communication complexity for the normal-case mode, to ensure high efficiency for small scales.

A chain-based idea, inspired by Bitcoin [47], has risen in the past five years. Using this idea, each consensus proposal (e.g., a block) contains a reference link to its parent. Thus, the confirmation on one proposal is equivalent to the confirmation on all its preceding proposals. When combined with the elegant pipelining, implicitly described in Casper [13] to piggyback the second round of voting on the next block's voting, the total communication cost can be amortized and the average voting round can be reduced to one. Several recent works

[11], [12], [58], [53], [16] adopt these ideas to improve the efficiency. In particular, HotStuff adopts both ideas and follows the framework of Tendermint [11], [12] and Casper [13], it achieves a linear view-change and optimistic responsiveness. However, the drawback of the protocols using the chain-based idea is that it requires consensus proposals to get confirmed in a sequential manner. Thus, those protocols lose the ability of the parallel execution which can be beneficial to increase resource utilization as well as efficiency. This is why we give up this idea when designing the view-change mode. We ensure a parallelly executed agreement during the normal-case mode since it happens most of the time. The communication cost for a view-change in our protocol is the same as LibraBFT [7], the consensus protocol of Facebook’s Diem [3].

After all of these efforts, the throughput of existing leader-based BFT protocols still drops significantly when the protocol’s scale increases. We observed (and verified in experiments) that the neglected but crucial data delivery step is the bottleneck for efficiency when the protocol’s scale is large. There are several other works [19], [55], [33] notify this. However, they bypassed the problem via leader-less BFT protocols [19], [55], [46], [31]. We elaborately analyzed and locates the step that gets stuck (§I). We amortized the cost of the leader by taking full advantage of the idle bandwidth resources of other replicas, which gives us a solution that confronts this problem directly. Experiment shows that our solution is effective. We were made aware of a concurrent work [21] which appeared recently. [21] identifies the critical path of consensus as in this paper, and it presents a protocol to deal with the data dissemination. However, [21] targets on designing a BFT protocol with a better throughput. In contrast, Leopard aims at preserving the efficiency when the protocol’s scale increases.

Table IV compares the communication complexity of Leopard to some of its most prominent alternatives. The comparison is limited in the normal-case mode where the leader is honest since the high efficiency of those protocols mainly comes from this mode. It shows that Leopard preserves the linear communication of the protocol overall and reduces the cost to the leader. The communication complexity of each replica in Leopard remains constant with respect to n . Hence, the protocol will not get stuck at some specific node when the scale increases.

TABLE IV. COMPARISON OF THE COMMUNICATION COMPLEXITY WHEN THE LEADER IS HONEST.

Protocol	Communication complexity			Responsiveness
	Total	Leader	Non-leader	
PBFT [15]	$O(n^2)$	$O(n)$	$O(n)$	yes
Tendermint [12]	$O(n^2)$	$O(n)$	$O(n)$	no
Casper [13]	$O(n^2)$	$O(n)$	$O(n)$	no
SBFT [29]	$O(n)$	$O(n)$	$O(1)$	yes
HotStuff [58]	$O(n)$	$O(n)$	$O(1)$	yes
Leopard	$O(n)$	$O(1)$	$O(1)$	yes

The idea of decoupling consensus proposals is not new. There are several blockchain protocols, such as Bitcoin-NG [25], ByzCoin [38] and Prism [6], have adopted this idea to improve efficiency. In particular, Prism [6] presents an excellent blockchain protocol based on Bitcoin by deconstructing

blocks to obtain a smaller block size thus shortens the block interval and increases the efficiency. Leopard is inspired by this technique but with a different purpose. It aims at balancing the workload of replicas and removing the bottleneck of the leader-based BFT protocol. Besides, Leopard is a BFT protocol that provides deterministic safety and liveness guarantees. The above blockchain protocols, however, can only provide probabilistic security that may be exploited by adversaries to cause confusion, fraudulent transactions and distrust [40], [26], [34].

There are other techniques to balance the workload of a specific node on disseminating messages, for example, the broadcast tree [56] and the reliable broadcast (RBC) with erasure codes [14]. When using the broadcast tree to do the dissemination, replicas establish a tree on which each node resides a replica and the sender is on the root. A message is delivered from the root downward layer-by-layer, and each replica only has to deliver the message to its children. However, when all replicas are honest, it still costs $O(\log n)$ time complexity per message delivery. Even worse, this technique is quite susceptible to faults, since any Byzantine node can simply stop passing the message to its children, letting all replicas reside on the subtree rooted by the Byzantine node fail to receive the message. In addition, the well-known RBC with erasure codes scheme [14] used in many existing protocols [46], [31] has a communication complexity of $O(n|M| + \kappa n^2 \log n)$ where κ is the security parameter and $|M|$ is the message size. Although it has been improved by removing the $\log n$ item, the quadratic communication complexity is still not friendly to support a large scale of replicas. Besides, the message size $|M|$ in [14] is $\Omega(n \log n)$ due to the usage of erasure codes. This means the batch size is excessively large with a large n , and no tradeoff between throughput and latency is possible as in ours.

VII. CONCLUSION

The scalability and efficiency are two key metrics for a practical BFT protocol. However, the throughput of most existing leader-based BFT protocols drops significantly as the scale increasing. They thus face a scalability-efficiency dilemma. In this paper, we analyzed the bottleneck to this problem and defined a new metric called “scaling factor” to capture whether a BFT protocol can preserve the efficiency when the number of replicas increases. We presented a leader-based BFT protocol called “Leopard”. Our protocol enables preserving high throughput when the scale grows. It obtains the ideal scaling factor that is constant to n , and supports a more effective scaling up with 1/2 improvement of throughput by doubling the configured bandwidth at each replica. This is achieved by amortizing the workload of the leader to other replicas and taking full advantage of the idle resources. We conducted a variety of experiments on the implementation of Leopard with up to 600 replicas. The evaluation shows the throughput of Leopard remains almost flat at 10^5 and it achieves significant multi-sided performance improvements to the state-of-the-art BFT solution, HotStuff.

REFERENCES

[1] M. Abd-El-Malek, G. R. Ganger, G. R. Goodson, M. K. Reiter, and J. J. Wylie, “Fault-Scalable Byzantine Fault-Tolerant Services,” in *Proceedings of the Twentieth ACM Symposium on Operating Systems Principles*, ser. SOSP ’05. ACM, 2005, pp. 59–74.

[2] Y. Amir, B. A. Coan, J. Kirsch, and J. Lane, “Prime: Byzantine Replication under Attack,” *IEEE Trans. Dependable Secur. Comput.*, vol. 8, no. 4, pp. 564–577, 2011.

[3] D. Association, “The Diem: To build a trusted and innovative financial network that empowers people and businesses around the world,” <https://www.diem.com/en-us/>, 2021.

[4] AWS, “AWS Outbound Data Transfer Prices Reduced By \$0.02/GB,” 2010. [Online]. Available: <https://aws.amazon.com/cn/blogs/aws/aws-data-transfer-prices-reduced/>

[5] M. Azure, “Bandwidth Pricing Details,” 2020. [Online]. Available: <https://azure.microsoft.com/en-us/pricing/details/bandwidth/>

[6] V. Bagaria, S. Kannan, D. Tse, G. Fanti, and P. Viswanath, “Prism: Deconstructing the Blockchain to Approach Physical Limits,” in *Proceedings of the 2019 ACM SIGSAC Conference on Computer and Communications Security*, ser. CCS ’19. ACM, 2019, pp. 585–602.

[7] M. Baudet, A. Ching, A. Chursin, G. Danezis, F. Garillot, Z. Li, D. Malkhi, O. Naor, D. Perelman, and A. Sonnino, “State Machine Replication in the Libra Blockchain,” *The Libra Assn. Tech. Rep.*, 2019.

[8] A. N. Bessani, J. Sousa, and E. A. P. Alchieri, “State Machine Replication for the Masses with BFT-SMART,” in *44th Annual IEEE/IFIP International Conference on Dependable Systems and Networks*, ser. DSN’14. IEEE, 2014, pp. 355–362.

[9] A. Boldyreva, “Threshold Signatures, Multisignatures and Blind Signatures Based on the Gap-Diffie-Hellman-Group Signature Scheme,” in *Public Key Cryptography — PKC 2003*. Springer, 2003, pp. 31–46.

[10] D. Boneh, B. Lynn, and H. Shacham, “Short Signatures from the Weil Pairing,” in *Advances in Cryptology — ASIACRYPT 2001*. Springer, 2001, pp. 514–532.

[11] E. Buchman, “Tendermint: Byzantine Fault Tolerance in the Age of Blockchains,” Ph.D. dissertation, 2016.

[12] E. Buchman, J. Kwon, and Z. Milosevic, “The latest gossip on bft consensus,” *CoRR*, vol. abs/1807.04938, 2018. [Online]. Available: <http://arxiv.org/abs/1807.04938>

[13] V. Buterin and V. Griffith, “Casper the Friendly Finality Gadget,” *CoRR*, vol. abs/1710.09437, 2017. [Online]. Available: <http://arxiv.org/abs/1710.09437>

[14] C. Cachin and S. Tessaro, “Asynchronous Verifiable Information Dispersal,” in *24th IEEE Symposium on Reliable Distributed Systems (SRDS’05)*. IEEE, 2005, pp. 191–201.

[15] M. Castro and B. Liskov, “Practical Byzantine Fault Tolerance,” in *Proceedings of the Third Symposium on Operating Systems Design and Implementation*, ser. OSDI ’99. USENIX Association, 1999, pp. 173–186.

[16] B. Y. Chan and E. Shi, “Streamlet: Textbook Streamlined Blockchains,” Cryptology ePrint Archive, Report 2020/088, 2020, <https://eprint.iacr.org/2020/088>.

[17] T.-H. H. Chan, R. Pass, and E. Shi, “PaLa: A Simple Partially Synchronous Blockchain,” Cryptology ePrint Archive, Report 2018/981, 2018, <https://eprint.iacr.org/2018/981>.

[18] R. Chen and J.-M. Park, “Attack Diagnosis: Throttling Distributed Denial-of-Service Attacks Close to the Attack Sources,” in *Proceedings. 14th International Conference on Computer Communications and Networks. 2005. ICCCN 2005*. IEEE, 2005.

[19] T. Crain, C. Natoli, and V. Gramoli, “Red Belly: A Secure, Fair and Scalable Open Blockchain,” 2021.

[20] I. Damgård and M. Koprowski, “Practical Threshold RSA Signatures without a Trusted Dealer,” in *Advances in Cryptology — EUROCRYPT 2001*. Springer, 2001, pp. 152–165.

[21] G. Danezis, E. K. Kogias, A. Sonnino, and A. Spiegelman, “Narwhal and Tusk: A DAG-based Mempool and Efficient BFT Consensus,” 2021.

[22] S. Das, Z. Xiang, and L. Ren, “Asynchronous Data Dissemination and its Applications,” Cryptology ePrint Archive, Report 2021/777, 2021, <https://eprint.iacr.org/2021/777>.

[23] B. David, B. Magri, C. Matt, J. B. Nielsen, and D. Tschudi, “GearBox: An Efficient UC Sharded Ledger Leveraging the Safety-Liveness Dichotomy,” Cryptology ePrint Archive, Report 2021/211, 2021, <https://eprint.iacr.org/2021/211>.

[24] C. Dwork, N. Lynch, and L. Stockmeyer, “Consensus in the Presence of Partial Synchrony,” *J. ACM*, vol. 35, no. 2, pp. 288–323, 1988.

[25] I. Eyal, A. E. Gencer, E. G. Sirer, and R. van Renesse, “Bitcoin-NG: A Scalable Blockchain Protocol,” in *13th USENIX Symposium on Networked Systems Design and Implementation*, ser. NSDI ’16. USENIX Association, 2016, pp. 45–59.

[26] I. Eyal and E. G. Sirer, “Majority Is Not Enough: Bitcoin Mining Is Vulnerable,” in *Financial Cryptography and Data Security*. Springer, 2014, pp. 436–454.

[27] M. J. Fischer, N. A. Lynch, and M. Paterson, “Impossibility of distributed consensus with one faulty process,” in *Proceedings of the Second ACM SIGACT-SIGMOD Symposium on Principles of Database Systems*, ser. PODS ’83. ACM, 1983, pp. 1–7.

[28] Y. Gilad, R. Hemo, S. Micali, G. Vlachos, and N. Zeldovich, “Algordan: Scaling Byzantine Agreements for Cryptocurrencies,” in *Proceedings of the 26th Symposium on Operating Systems Principles*, ser. SOSP ’17. ACM, 2017, pp. 51–68.

[29] G. Golan-Gueta, I. Abraham, S. Grossman, D. Malkhi, B. Pinkas, M. K. Reiter, D. Seredinschi, O. Tamir, and A. Tomescu, “SBFT: A Scalable and Decentralized Trust Infrastructure,” in *49th Annual IEEE/IFIP International Conference on Dependable Systems and Networks*, ser. DSN’19. IEEE, 2019, pp. 568–580.

[30] R. Guerraoui, “The Next 700 BFT Protocols,” in *Principles of Distributed Systems*. Springer, 2008, pp. 1–1.

[31] B. Guo, Z. Lu, Q. Tang, J. Xu, and Z. Zhang, “Dumbo: Faster Asynchronous BFT Protocols,” in *Proceedings of the 2020 ACM SIGSAC Conference on Computer and Communications Security*, ser. CCS ’20. Association for Computing Machinery, 2020, p. 803–818.

[32] J. Göbel and A. Krzesinski, “Increased Block Size and Bitcoin Blockchain Dynamics,” in *2017 27th International Telecommunication Networks and Applications Conference (ITNAC)*. IEEE, 2017.

[33] F. P. Junqueira, B. C. Reed, and M. Serafini, “Zab: High-Performance Broadcast for Primary-Backup Systems,” in *Proceedings of the 2011 IEEE/IFIP International Conference on Dependable Systems and Networks*, ser. DSN’11. IEEE, 2011, pp. 245–256.

[34] G. O. Karame, E. Androulaki, and S. Capkun, “Double-Spending Fast Payments in Bitcoin,” in *Proceedings of the 2012 ACM Conference on Computer and Communications Security*, ser. CCS ’12. ACM, 2012, pp. 906–917.

[35] M. Kelkar, F. Zhang, S. Goldfeder, and A. Juels, “Order-Fairness for Byzantine Consensus,” in *Annual International Cryptology Conference*. Springer, 2020, pp. 451–480.

[36] A. Kiayias and A. Russell, “Ouroboros-BFT: A Simple Byzantine Fault Tolerant Consensus Protocol,” Cryptology ePrint Archive, Report 2018/1049, 2018, <https://eprint.iacr.org/2018/1049>.

[37] E. Kokoris-Kogias, P. Jovanovic, L. Gasser, N. Gailly, E. Syta, and B. Ford, “OmniLedger: A Secure, Scale-Out, Decentralized Ledger via Sharding,” in *2018 IEEE Symposium on Security and Privacy (SP)*, 2018, pp. 583–598.

[38] E. Kokoris-Kogias, P. Jovanovic, N. Gailly, I. Khoffi, L. Gasser, and B. Ford, “Enhancing Bitcoin Security and Performance with Strong Consistency via Collective Signing,” in *25th USENIX Security Symposium*. USENIX Association, 2016, pp. 279–296.

[39] R. Kotla, L. Alvisi, M. Dahlin, A. Clement, and E. L. Wong, “Zyzzyva: Speculative Byzantine Fault Tolerance,” in *Proceedings of Twenty-First ACM SIGOPS Symposium on Operating Systems Principles*, ser. SOSP ’07. ACM, 2007, pp. 45–58.

[40] Y. Kwon, D. Kim, Y. Son, E. Vasserman, and Y. Kim, “Be Selfish and Avoid Dilemmas: Fork After Withholding (FAW) Attacks on Bitcoin,” in *Proceedings of the 2017 ACM SIGSAC Conference on Computer and Communications Security*, ser. CCS ’17. ACM, 2017, p. 195–209.

[41] L. Lamport, R. E. Shostak, and M. C. Pease, “The Byzantine Generals Problem,” *ACM Trans. Program. Lang. Syst.*, vol. 4, no. 3, pp. 382–401, 1982.

[42] K. Li, J. Chen, X. Liu, Y. Tang, X. Wang, and X. Luo, “As Strong As Its Weakest Link: How to Break Blockchain DApps at RPC Service,” in *28th Annual Network and Distributed System Security Symposium, NDSS 2021*. The Internet Society, 2021.

[43] F. Ludovici and H. P. Pfeifer, “NetEm - Network Emulator,” 2011. [Online]. Available: <https://www.linux.org/docs/man8/tc-netem.html>

[44] L. Luu, V. Narayanan, C. Zheng, K. Baweja, S. Gilbert, and P. Saxena, “A Secure Sharding Protocol For Open Blockchains,” in *Proceedings of*

the 2016 ACM SIGSAC Conference on Computer and Communications Security, ser. CCS '16. ACM, 2016, pp. 17–30.

[45] J. Martin and L. Alvisi, “Fast Byzantine Consensus,” in *2005 International Conference on Dependable Systems and Networks*, ser. DSN'05. IEEE, 2005, pp. 402–411.

[46] A. Miller, Y. Xia, K. Croman, E. Shi, and D. Song, “The Honey Badger of BFT Protocols,” in *Proceedings of the 2016 ACM SIGSAC Conference on Computer and Communications Security*, ser. CCS '16. ACM, 2016, pp. 31–42.

[47] S. Nakamoto, “Bitcoin: A Peer-to-Peer Electronic Cash System,” <https://bitcoin.org/bitcoin.pdf>, 2008.

[48] K. Nayak, L. Ren, E. Shi, N. H. Vaidya, and Z. Xiang, “Improved Extension Protocols for Byzantine Broadcast and Agreement,” in *34th International Symposium on Distributed Computing, DISC 2020*, ser. LIPIcs, vol. 179. Schloss Dagstuhl - Leibniz-Zentrum für Informatik, 2020, pp. 28:1–28:17.

[49] R. Pass and E. Shi, “Hybrid Consensus: Efficient Consensus in the Permissionless Model,” in *31st International Symposium on Distributed Computing, DISC 2017*, ser. LIPIcs, vol. 91. Schloss Dagstuhl - Leibniz-Zentrum für Informatik, 2017, pp. 39:1–39:16.

[50] M. C. Pease, R. E. Shostak, and L. Lamport, “Reaching Agreement in the Presence of Faults,” *J. ACM*, vol. 27, no. 2, pp. 228–234, 1980.

[51] F. B. Schneider, “Implementing Fault-Tolerant Services Using the State Machine Approach: A Tutorial,” *ACM Comput. Surv.*, vol. 22, no. 4, pp. 299–319, 1990.

[52] D. Schwartz, N. Youngs, A. Britto *et al.*, “The Ripple Protocol Consensus Algorithm,” *Ripple Labs Inc White Paper*, vol. 5, no. 8, p. 151, 2014.

[53] E. Shi, “Streamlined Blockchains: A Simple and Elegant Approach (A Tutorial and Survey),” in *Advances in Cryptology – ASIACRYPT 2019*. Springer, 2019, pp. 3–17.

[54] V. Shoup, “Practical threshold signatures,” in *Advances in Cryptology – EUROCRYPT 2000*. Springer, 2000, pp. 207–220.

[55] G. Voron and V. Gramoli, “Dispel: Byzantine SMR with Distributed Pipelining,” *CoRR*, vol. abs/1912.10367, 2019. [Online]. Available: <http://arxiv.org/abs/1912.10367>

[56] Wikipedia, “Two-tree broadcast,” 2020. [Online]. Available: https://en.wikipedia.org/wiki/Two-tree_broadcast

[57] ———, “HTTP persistent connection,” 2021. [Online]. Available: https://en.wikipedia.org/wiki/HTTP_persistent_connection

[58] M. Yin, D. Malkhi, M. K. Reiter, G. Golan-Gueta, and I. Abraham, “HotStuff: BFT Consensus with Linearity and Responsiveness,” in *Proceedings of the 2019 ACM Symposium on Principles of Distributed Computing*, ser. PODC '19. ACM, 2019, pp. 347–356.

[59] M. Yin, D. Malkhi, M. K. Reiter, G. G. Gueta, and I. Abraham, “Hotstuff: Bft consensus in the lens of blockchain,” 2019. [Online]. Available: <https://arxiv.org/abs/1803.05069v6>

[60] T. Yin, “libhotstuff,” <https://github.com/hot-stuff/libhotstuff>, 2019.

[61] M. Zamani, M. Movahedi, and M. Raykova, “RapidChain: Scaling Blockchain via Full Sharding,” in *Proceedings of the 2018 ACM SIGSAC Conference on Computer and Communications Security*, ser. CCS '18. ACM, 2018, pp. 931–948.

APPENDIX A

PROTOCOLS OF CHECKPOINT AND VIEW-CHANGE

The detailed checkpoint protocol for generating a checkpoint is presented in Algorithm 3.

Next, we present the view-change protocol. The protocol contains three steps: view-change trigger, leader rotation, and state synchronization. View-change trigger decides when to invoke the view-change protocol. Leader rotation appoints the identity of the new leader. State synchronization synchronizes the state of the current view among replicas to avoid safety-violation in the new view.

We adopt a simple round-robin policy as in [17], [29], [36] for the leader election, where the $(v \bmod n)$ -th replica is the

Algorithm 3 Making a checkpoint

```

1: for replica  $i$  do
2:   let  $sn$  be the serial number of the latest executed BFTblock
   and  $st$  be the related execution state
3:   if  $(sn \bmod k/2 = 0)$  then ▷ produce a checkpoint
4:      $cp \leftarrow \langle \text{checkpoint}, sn, H(st) \rangle$ 
5:      $\hat{\sigma}_i \leftarrow \text{TSig}(tsk_i, cp)$ 
6:     send  $(cp, \hat{\sigma}_i)$  to  $L_v$ 
7: for leader  $L_v$  do
8:   wait for  $2f + 1$  valid checkpoint messages
9:    $\hat{\sigma} \leftarrow \text{TSR}(\{\hat{\sigma}_j\}_{j=1}^{2f+1})$  ▷ create a proof for cp
10:  multicast  $(cp, \hat{\sigma})$  to all replicas
11: for replica  $i$  do
12:   if  $\text{TVrf}(tpk, \hat{\sigma}, cp) \rightarrow 1$  then
13:     update the maintained latest checkpoint message  $lc$  to  $(cp, \hat{\sigma})$ 
14:      $lw \leftarrow sn$  ▷ advance the lower water mark lw
15:   return accept

```

eligible leader of view v . The view-change trigger and state synchronization steps of the protocol are as follows:

- *View-change trigger*: A client randomly selects s replicas (like in the datablock preparation) and re-sents a timeout request to the chosen replicas, in which the honest replica will propagate the request (with a special tag) in a datablock. A replica starts a timer when it receives a re-sent request, either from the client or inside a datablock from another replica. The replica i triggers a view change either (1) a timer expires and no acknowledgment of the request have been sent, and in this case, i sends a timeout message $\langle \text{timeout}, v \rangle$, together with i 's signature on it, to all replicas, or (2) i receives a proof that the leader is faulty either via a publicly verifiable contradiction or when received $f + 1$ timeout messages from other replicas. The replica then stops executing the normal-case protocol (Algorithm 2 and 3) of the current view v . As in PBFT, it requires that the timer for triggering a view-change should be set appropriately. This is to avoid switching to a new view too frequently due to the actual network delay.

- *State synchronization*: Each replica i collects all notarized BFTblocks with a serial number higher than lw . Replica i sends a view-change message $m = \langle \text{view-change}, v + 1, lc, \mathcal{B} \rangle$, together with i 's signature on m , to the leader of the next view $v + 1$. \mathcal{B} is a set containing hashes of collected BFTblocks and their notarization proofs.

The next view leader L_{v+1} waits for $2f + 1$ valid view-change messages. L_{v+1} then multicasts a new-view message $\hat{m} = \langle \text{new-view}, v + 1, \mathcal{V} \rangle$, together with L_{v+1} 's threshold signature on \hat{m} , to all replicas. \mathcal{V} is the set of $2f + 1$ view-change messages.

When a valid view-change message is received, such that it is signed by the eligible leader and contains $2f + 1$ valid new-view messages, i advances to view $v + 1$. Replicas restart the normal-case mode under view $v + 1$ by first redoing the agreement for each BFTblock linked in \mathcal{V} without re-executing them. The empty position between BFTblocks is filled with a dummy BFTblock with empty content.

APPENDIX B SECURITY PROOFS

The protocol satisfies safety, captured in Theorem 3, and liveness, captured in Theorem 4. We first give and prove Lemma 1 and Lemma 2 before presenting the proof of safety.

Lemma 1 (Uniqueness). *Assume the threshold signature scheme is secure. If two BFTblocks B_1 and B_2 both with the same serial number are notarized in the same view, then it must be the case that $B_1 = B_2$.*

Proof: Since B_1 is notarized and by the definition of the protocol, there must be a set R containing $2f + 1$ distinct replicas who have signed B_1 ; otherwise, a reduction can be built to break the unforgeability of the threshold signature scheme. As there is at most f Byzantine replicas, at least $f + 1$ honest replicas are contained in R . Similarly, we have that at least $f + 1$ honest replicas have signed B_2 . Since there are $3f + 1$ replicas in total and by the pigeon-hole principle, at least one honest replica has signed both B_1 and B_2 . Since an honest replica will only sign one BFTblock with a specific serial number, it holds that $B_1 = B_2$. ■

Lemma 2. *For any serial number sn , if any two honest replicas have two BFTblocks with the serial number equals to sn in their output logs, the contents of the two BFTblocks are the same.*

Proof: We denote the two BFTblocks from the two honest replicas' logs as B and B' , respectively. Due to Lemma 1, if B and B' are added into the logs in the same view, then it holds $B = B'$. We now consider the case that they are added into the logs in different views v and v' , respectively. W.l.o.g., we assume $v < v'$.

Following Algorithm 2 (line 40), B (resp. B') is added into the log in view v (resp. v') since it gets confirmed. Hence, there must be $2f + 1$ replicas knows that B (resp. B') is notarized. If the serial number of B is lower than the lower watermark lw , the execution state after B has been included in the latest checkpoint message. Hence, an honest replica will never accept a different BFTblock from B with the serial number sn following Algorithm 2 (line 15). Otherwise, since the new-view message for advancing to view v' contains $2f + 1$ view-change messages and there are at most f Byzantine replicas, at least one honest replica i satisfies (1) B is notarized at i , and (2) the new-view message contains the view-change message from i . Hence, the protocol will redo the B in view v' with the same serial number sn , only with a new view number v' . Hence, the contents of B and B' remains the same. ■

Theorem 3 (Restatement of Theorem 1). *If two distinct requests exist on the same position of two output logs, then the two logs cannot be both from honest replicas.*

Proof: Since a BFTblock contains links to datablocks and each datablock contains requests, Theorem 3 follows directly from Lemma 2. ■

Due to the FLP impossibility [27], the liveness of Leopard relies on the synchronous assumption, where synchrony is achieved after GST in the standard partially synchronous network model adopted in this paper.

Theorem 4 (Restatement of Theorem 2). *After GST, the confirmation for a pending request must be completed.*

Proof: In the optimistic case that both the leader and the replica i who receives a pending request req from the client are honest, the leader will link the datablock sent by i , which contains req , into a BFTblock. After a period of another 5Δ , the BFTblock that logically links req will be confirmed hence req gets confirmed too.

If the replica i is faulty and it ignores req , the client will re-send req to at most $f + 1$ replicas within which at least one honest replica exists who will disseminate req in a newly generated datablock to all replicas including the leader. This then reduces to the optimistic case in the above.

If the leader is faulty and it ignores datablocks containing req when generating a BFTblock, the re-sent request will trigger a view-change due to the timeout mechanism in the view-change protocol. Since there is at most f Byzantine replicas, after at most another $f - 1$ new views, there must be a view with an honest leader. This then reduces to the above case. ■

APPENDIX C MORE DETAILS ABOUT THE EXPERIMENTS

A. Experimental Results on Varying the Batch Sizes

We present the detailed experimental results on the measures of batch sizes with a varying n for both our system and HotStuff.

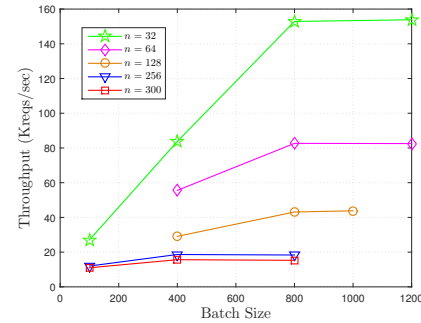


Fig. 11. Throughput of HotStuff on varying batch sizes.

Notice that in HotStuff, as well as other BFT solutions, there is only one batch and it is for batching requests into a consensus proposal (i.e., a block). Fig. 11 depicts the throughput with different batch sizes for five replica numbers (32, 64, 128, 256, 300) in HotStuff. Results show that throughput goes up as we increase the batch size, but it stops to grow after a certain batch size value. We let the batch size at this point be the implementation parameter of HotStuff. We remark that, the latency still goes up if we keeps increasing the batch size.

Different from HotStuff, there are two batch sizes in our system, namely BFTblock size (or BFTsize) and datablock size (or α). We varied one batch sizes while fixing the other one at different n between 32 and 600. Fig. 12 depicts the throughput and latency of our system with different datablock sizes and BFTsizes when $n = 64$ as an example. We use a red box in Fig. 12 to show the batch size we choose after balancing

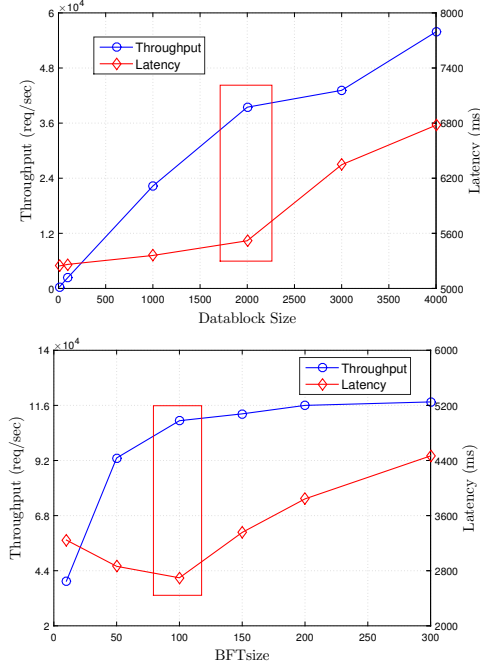


Fig. 12. Performance of our system on varying batch sizes with $n = 64$.

the throughput and the latency. Since the results with other n values present a similar tendency to $n = 64$, we omit the experimental results.